JOURNAL OF MATERIALS SCIENCE 22 (1987) 4292–4298

Effects of structure on the tensile, creep and fatigue properties of polyester fibres

Ch. OUDET*, A. R. BUNSELL
Ecole Nationale Supérieure des Mines de Paris, Centre des Matériaux, B.P. 87, 91003 Evry Cédex, France

The behaviour of two types of polyester fibres have been compared and the differences observed explained in terms of the differences in molecular structure. One fibre which had a higher crystallinity than the other showed improved creep behaviour however shorter fatigue lifetime. Crack propagation during fatigue suggests a macrofibrillar structure superimposed on the microfibrillar molecular arrangement. Fatigue lifetime is suggested as being greatly influenced by the time necessary for crack initiation which involves modification of the molecular structure. The influence of the minimum cyclic load on fatigue lifetime has been studied for both fibres.

1. Introduction

Polyethylene terephthalate fibres, abbreviated in this paper to polyester fibres, are used for a wide variety of applications other than traditional textile uses. Many of the industrial uses to which polyester fibres are put subject them to prolonged loading and very often to fatigue conditions. In order to optimize fibre behaviour it is necessary to understand the processes occurring at the molecular level which determine behaviour under load. Although considerable insight had been gained into fibre behaviour and structure before the development of the scanning electron microscope (SEM) the ability to examine closely the fracture morphology of fine fibres stimulated and aided the study of the relationship between fibre structure and properties [1, 2]. Tensile and creep failure of these fibres has been seen to involve crack initiation at the fibre surface, slow propagation normal to the fibre axis and simultaneous opening of the crack due to plastic deformation ahead of the crack tip, followed by rapid failure. This leads to two very similar fracture ends and a distinctive tensile fracture morphology [1]. A distinct fatigue process has been shown to occur in polyester fibres when they are subjected to certain cyclic tensile loading conditions. Fatigue failure in both polyester and polyamide fibres leads to a distinctive fracture morphology involving crack growth along the fibre at a slight angle to the fibre axis [3, 4]. Ultimate failure occurs when the load bearing cross section is sufficiently reduced so as to initiate creep failure under the applied load. It was shown that a necessary criterion for fatigue failure was a sufficiently low minimum cyclic load [4, 5]. More recent studies have shown that the development of fatigue failure in polyester fibres is associated with a localized fall in crystallinity within the fibre structure [6]. An amorphous band is created within the fibre and gradually penetrates in towards the fibre centre. Micropores develop within this band which, on coalescence, develop into the fatigue crack which propagates along the amorphous band to give rise to the distinctive fatigue fracture morphology.

The present study considers two samples of very similar polyester fibres but differing in their microstructures due to differing heat treatment histories. The influence of the differences in structures on the fibre properties has been examined and the role of the structure determining the mechanical properties discussed.

2. Experimental details

2.1. Fibre characteristics

The fibres which have been examined were obtained from two samples of industrial fibres manufactured by Viscosuisse (Rhone, Poylenc, Switzerland) and destined for use as reinforcements in rubber. The fibres were cylindrical with a generally smooth surface with occasional protuberances attributed to the diffusion of oligomer elements [7]. The two samples of fibre have been called, arbitrarily, for the purposes of this study, 2 GTA and 2 GTB. Their physical characteristics are given in Table I.

2.2. Mechanical Tests

All tests were conducted on single fibres with the aid of a Universal Fibre Tensile tester which has been described elsewhere [8]. The machine consists of two jaws which grip the fibre to be tested. One jaw is attached to a moveable cross head controlled by an electric motor which, under load controlled conditions operates so as to maintain the load on the fibre constant. The load is monitored by means of two transducers which measure the mean load and the amplitude of any cyclic load. In the case of a fatigue

Present address: Lab. de Polymères, Ecole Polytechnique Fédérale de Lausanne, 32 Chemin de Bellerive, CH-1007 Lausanne, Switzerland.

0022–2461/87 $03.00 + .12

TABLE I Characteristics of the two types of fibre studied

	2 GTA	2 GTB
Fibre diameter	23.6 (±1.7) μm	22.7 (±1.6) μm
Linear mass	5.39 (±0.38) d tex	5.21 (±0.34) d tex

test an electromagnetic vibrator, to which the other grip is attached, provides a sinusoidal movement. The frequency used in these fatigue tests was 50 Hz and the gauge length was 50 mm. Fatigue tests were usually stopped after 10^7 cycles if failure had not occurred. All tests were conducted under conditions of 50% relative humidity and at 23° C.

2.3. Microstructure

The microstructure of semi-crystalline organic fibres has generated considerable speculation. Peterlin suggested that drawn fibres were made up of orientated microfibrils consisting of alternating regions of amorphous and well ordered material [9]. Prevorsek developed the microfibrillar model and proposed the existence of three phases; a crytstalline phase, an amorphous intrafibrillar phase and an interfibrillar oriented amorphous phase which we shall call the mesomorphous phase [10].

The structure of the two types of fibres which have been studied were revealed by Sotton using X-ray diffraction and the results obtained are shown in Table II [11]. The measured factors are defined as:

(a) true crystallinity, which takes into account the disorder factor as described by Sotton [12].

(b) disorder factor, which is calculated using the theory of Ruland which takes into account structural distortions [13].

(c) crystallinity index, calculated as described by Statton using two standards, one 100% amorphous and the other 100% crystalline [14].

(d) crystalline volume, calculated from the 2θ spread of the 1 0 0, 0 1 0 and 1 0 5 bands.

(e) long period, which is the mean distance between the centre of two crystallites parallel to the fibre axis.

(f) length of amorphous zones parallel to the fibre axis, taken to be the difference between the long period and the height of the crystallites.

(g) small angle diffraction intensity expressed in arbitrary units with respect to the value R of the 2 GTB specimen.

The microstructural analysis was completed by differential scanning calorimetry and thermomechanical analysis. The principal differences between the two types of fibres are summarized in Table III and shown schematically in Fig. 1.

TABLE II Structural characteristics obtained by X-ray diffraction of the two fibres as obtained by Sotton [11]

	2 GTA	2 GTB
True Crystallinity (X_c)	0.35	0.25
Disorder factor (k)	2.9	2.5
Crystallinity index (%)	50.5	2.5
Crystallite volume (nm^3)	189	111
Long period (nm)	15	13.8
Length of amorphous zones (nm)	8.2	7.7
Small angle intensity (arbitrary units)	$R \times 3.6$	R

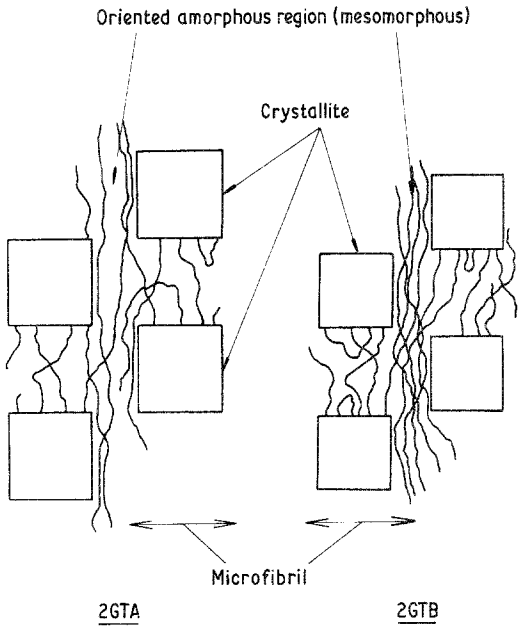

Figure 1 Schematic view of the molecular structure of the two types of fibres with the fibre axis vertical.

3. Experimental results

The load-strain curves for each type of fibre are shown in Fig. 2. Similar behaviour was observed with both fibres at small strains and a Young's modulus of 18 GPa was measured. Strain hardening was seen at greater strains and this was more marked with the 2 GTB specimens.

Under steady loading conditions both fibres were seen to creep as shown in Fig. 3. The creep rate was observed to gradually fall and to be a logarithmic function of time at low loads giving parallel curves for both specimens. At higher loads the creep rate was seen to increase prior to failure for both fibres. The fracture morphologies of the fibres broken in tension and in creep were similar and are shown in Figs 4 and 5.

Fatigue tests revealed similar fracture morphologies for both fibres and correspond to those previously described as indicative of the fatigue process [4, 6]. Such a fatigue failure is shown in Fig. 6. It should be noted that, as is usual for polyester fibres, final failure occurred behind the tip of the fatigue crack. The penetration of the fatigue crack into the fibre was studied by cutting the fibre into slices of about 1 μm thickness and measuring the reduction in section with the aid of an image analyzer. Considerable differences were seen in the rate of crack penetration even between

TABLE III Principal structural differences of the two fibre samples

	2 GTB	2 GTA
Crystalline phase	Crystallites regular in shape but small.	Crystallites large but irregular at the interface with the amorphous zone.
Non crystalline phase	High density	Low density

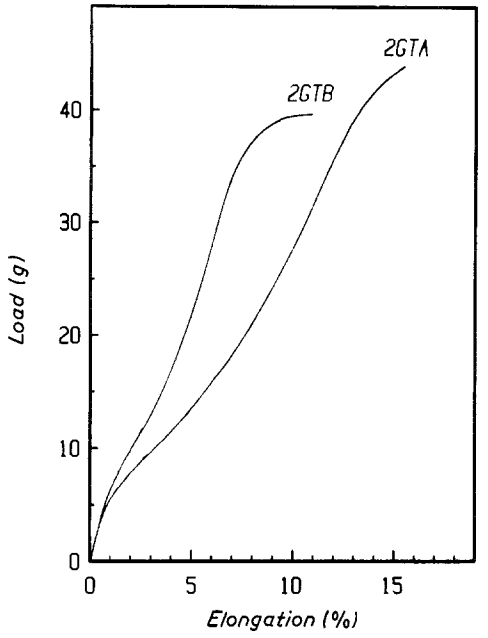

Figure 2 Load-elongation curves of the two types of fibres.

fibres of the same type as is illustrated by Figs 7 and 8 which correspond to two 2 GTA fibres taken from the same continuous monofilament and tested under the same conditions. It can be seen that crack growth in the fibre, A, remained for a long time parallel to the fibre axis and that the cross sectional shape of the crack was different when compared to fibre B. Fig. 9 shows striated fatigue fracture surface typical of that observed with both the 2 GTA and 2 GTB fibres. This was observed with both types of fibre although the fatigue cracks were usually wider with the 2 GTA fibres.

4. Discussion

The load elongation curves for the two types of fibres shown in Fig. 2 reveal very similar behaviour at low

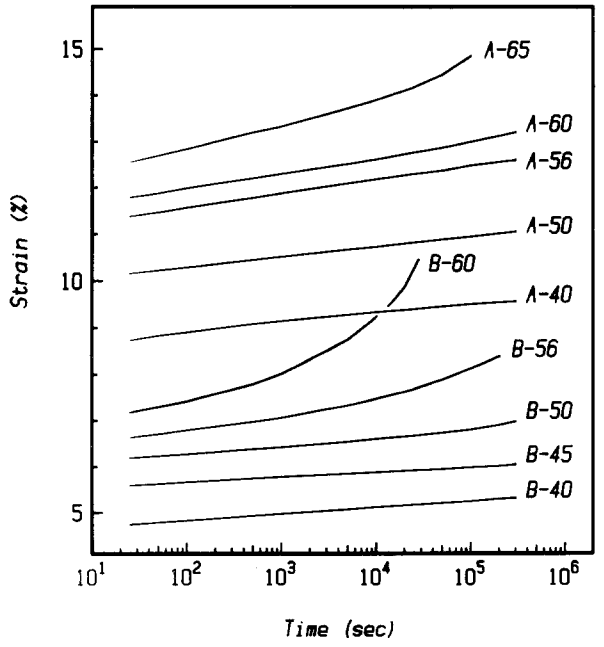

Figure 3 Comparison of the creep behaviour of the two polyester fibre types. B-60 indicates a 2 GTB fibre subjected to a load of 60 cN tex^{-1}.

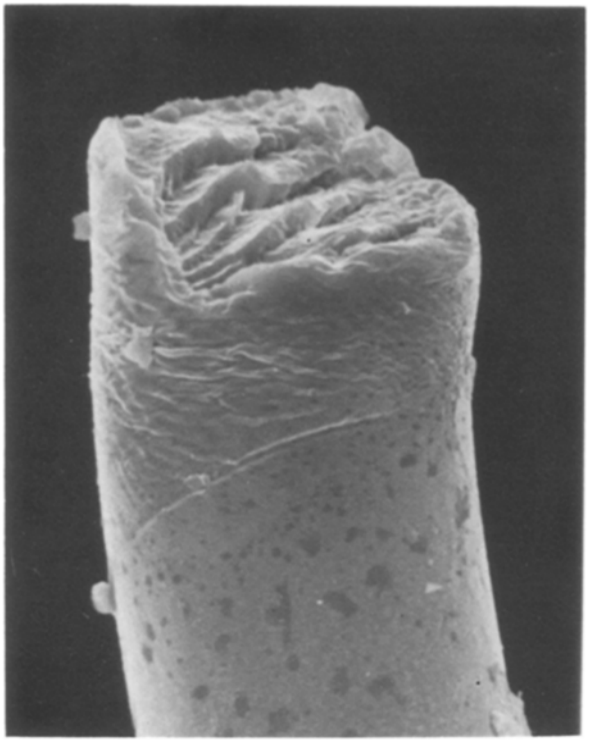

Figure 4 Fracture morphology of a 2 GTA fibre broken in creep.

strains at which only deformation of valence angles is occurring. At greater strains the increasing gradients which were observed suggest an improvement in the macromolecular orientation leading to an increase in the cohesion energy of the secondary bonds. This most probably indicates movement in the non-crystalline phases as the crystallites are already well compacted. This is in agreement with the interpretation of the microstructures given for the two fibres as the 2 GTB specimen possessed the non-crystalline phase with the

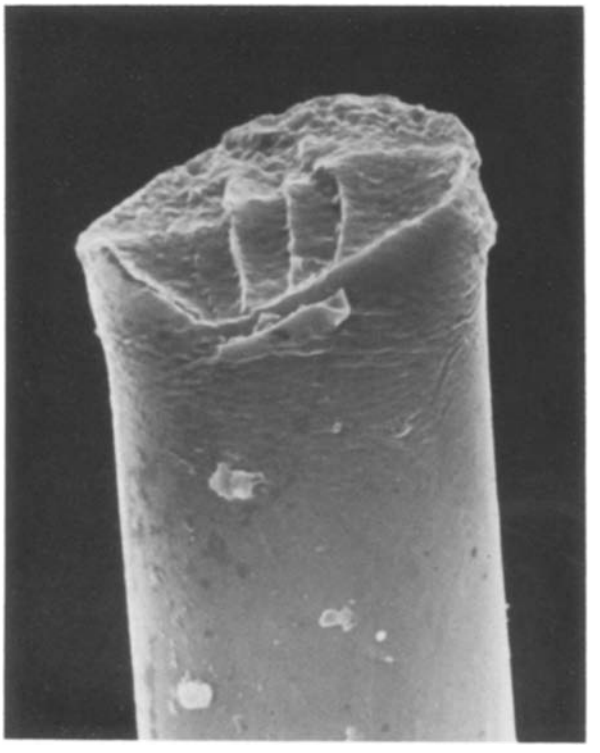

Figure 5 Fracture morphology of a 2 GTB fibre broken in creep.

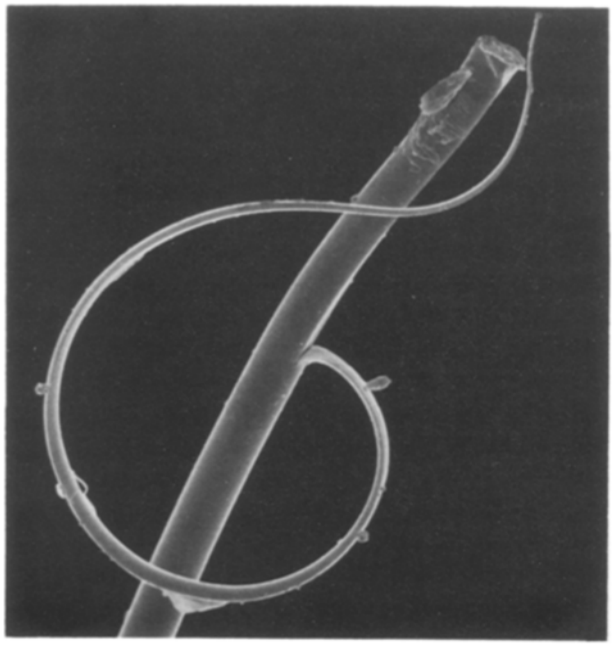

Figure 6 Fracture morphology of a 2 GTB fibre broken in fatigue.

greatest density and also showed the greatest strain hardening. The mesomorphous phase contains the most stretched molecules in the amorphous phases so that it is likely that it is this interfibrillar phase which controls strain hardening. Consequently the behaviour of the two fibres suggests that the 2 GTB fibres possessed a mesomorphous phase of greater density than that of the 2 GTA fibres.

After strain hardening of the fibres the molecules in the mesomorphous phases are highly stretched and it is possible that the failure occurs of some of those linking the crystallites both within microfibrils and between neighbouring microfibrils. The size of crystallites and the number of anchorage points of molecules from the mesomorphous phase is clearly an important factor in limiting damage and determining strength. Damage of this type accumulating within the fibre leads to a curvature in the load–strain curve which will be proportional to the degree of damage. This scenario was supported by the behaviour of the two fibres as the 2 GTA samples which possessed the largest crystallites showed only a slight curvature of the load–strain curve just before failure. The effect was much more marked with the 2 GTB fibres which

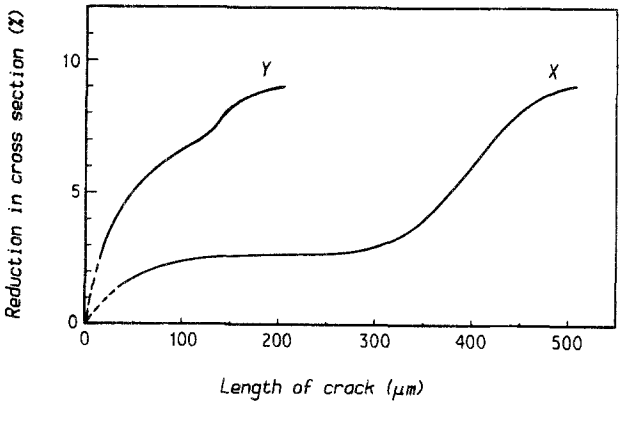

Figure 7 Two examples of the reduction of load bearing cross section during fatigue.

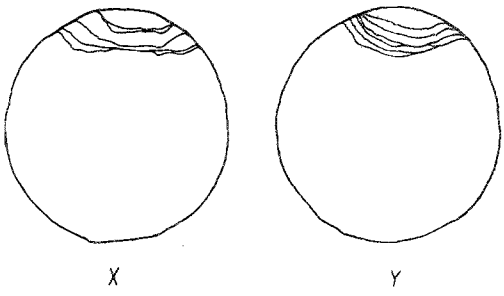

Figure 8 Penetration of the fatigue crack in Fig. 7 into the fibres.

possessed smaller crystallites. This can be confirmed by referring to Fig. 2 and Table IV. Crystallite size was not however the sole factor and it seems likely that the number of anchorage points on crystallites of mesomorphous molecules was greater in the 2 GTA fibres.

Behaviour under constant load for both fibres revealed a progressive fall in strain rate which can be explained by the stretching of the mesomorphous molecules as was seen to occur in simple tensile loading. The 2 GTA fibres showed a greater initial strain than did the 2 GTB fibres as should be expected as the former fibre possessed a lower density of the mesomorphous phase than did the latter fibre.

After the initial deformation both fibres showed similar linear increases in strain as a function of the logarithm of time as shown in Fig. 3. The similar behaviour suggests that the molecules in the mesomorphous phases become compacted under the applied load and attain similar densities.

Strain rate was seen to increase at high loads before failure, indicating damage accumulation in the fibre. This occurred much more quickly, under the same load, for the 2 GTB fibres due to their smaller crystallites which facilitated rupture of intra and interfibrillar linking molecules under creep and simple tensile loading. It seems therefore that much the same mechanisms were involved in creep as were found in simple tensile loading, as was suggested by the similar fracture morphologies obtained. It has however been suggested that the micro-structural arrangement of fibres can retard or accelerate the deformation processes [15]. Ultimate failure has been shown to

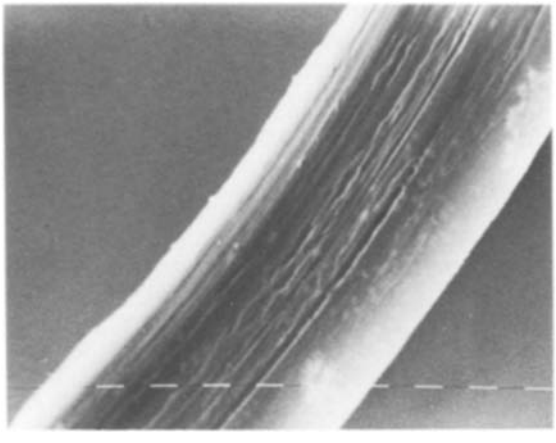

Figure 9 Fracture surface of a fatigued fibre revealing longitudinal striations. The lines represent 1 μm.

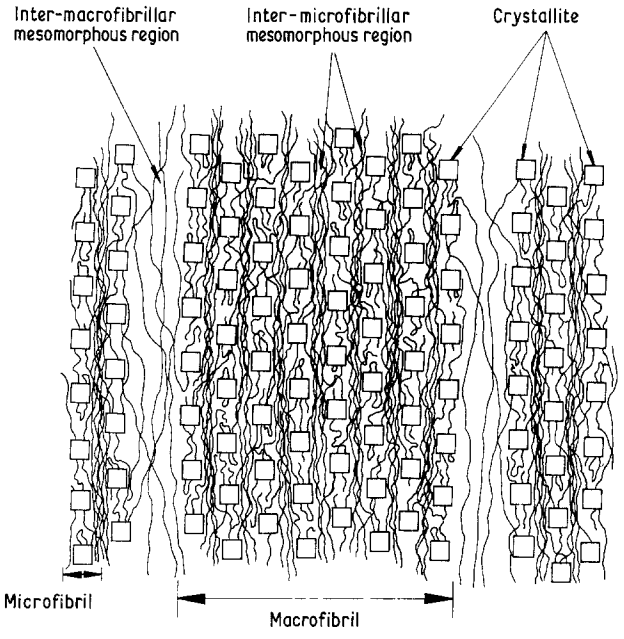

Figure 10 Schematic representation of the macro and microfibrillar structure of polyester fibres. The fibre axis is vertical.

occur by the fracture of macromolecular chains at C–C bonds in ethylene–glycol residue and results in the creation of free radicals [16].

The fracture surface of fatigued fibres, as can be seen in Fig. 9, or of fibres which have had their surfaces peeled back have a striated appearance suggesting a macrofibrillar structure superimposed on the microfibrils. The macrofibrils appear to take the form of cylinders with diameters of between 200 and 500 nm whilst the microfibrils have estimated diameters of 15 to 20 nm. The macro- and microfibrillar structure is illustrated schematically in Fig. 10 and can be applied to both types of fibres studied. The macrofibrillar structure of the fibres must considerably influence fatigue crack growth. Penetration of the fatigue crack into the fibre would be an irregular occurrence at faults or at the endings of macrofibrils. This view is supported by the curves of crack penetration shown in Fig. 7 and by the variation of crack front shape shown in Fig. 8.

Survival histograms shown in Fig. 11 for both types of fibres subjected to identical fatigue loading conditions revealed a significant difference in survival times. The 2 GTA fibres showed a lower value of median fatigue lifetime than did the 2 GTB fibres, which lasted three times longer. This was surprising as the tensile and creep tests revealed more rapid damage which was greater in extent with the 2 GTB fibres than with the 2 GTA specimens, as Figs 2 and 3 reveal.

TABLE IV Comparison of characteristics obtained in simple tensile loading

	2 GTA	2 GTB
Strain rate (% mm^{-1})	40	40
Number of specimens	100	50
Time to failure (sec)	23.1	15.9
Load at failure (g)	43.4 (±5.9)	39.7 (±2.7)
Fibre tenacity (N tex^{-1})	0.79	0.75
Strain to failure (%)	15.4 (±2.2)	10.6 (±2.2)
Stress at failure (MPa)	965 (±89)	964 (±131)

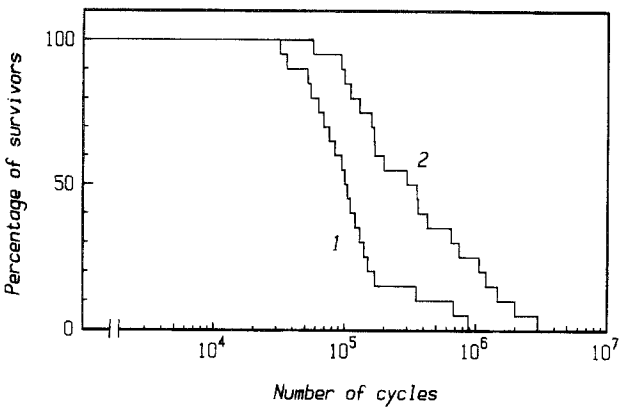

Figure 11 Cumulative histograms of fatigue lifetimes of the two fibres subjected to the same stress. (1) 2 GTA (0–57 cN tex^{-1}), (2) 2 GTB (0–57 cN tex^{-1}).

Reducing the maximum cyclic load on the fibre from 60% R to 53% but maintaining a zero minimum load produced an important increase in fatigue lifetime and an increase in the length of fatigue crack of around ten times.

The effect of minimum load on strain to failure under fatigue conditions is shown in Fig. 12 compared to the strain to failure under steady load conditions. It was observed that there was very little scatter of the strain to failure results under steady loads and that the results obtained in fatigue were clearly outside this scatter band. Strain to failure under conditions which led to fatigue failure was significantly greater than the strains recorded under steady loaded as shown in Table V. The strain to failure under fatigue conditions was seen to fall however as the minimum cyclic load was increased, until at around the minimum load threshold level the fatigue and creep strains to failure were similar. The median fatigue lifetimes of fibres were seen to increase dramatically as the minimum cyclic load was increased as is shown in Fig. 13. The differences in fatigue behaviours of the two fibre types is again shown in Fig. 14 which reveals that the same median lifetime was obtained when the minimum cyclic load was approximately five times higher for the 2 GTA fibre than with the 2 GTB fibre.

The fatigue lifetime of a specimen depends principally on three factors:

– time for crack initiation
– speed of crack propagation
– shape of the crack front reducing the load bearing cross section.

It seems that of these three factors it is the time for crack initiation which is likely to be the most important in determining total fatigue lifetimes. The 2 GTB fibres were found to have considerably longer

TABLE V Average strain to failure under creep and fatigue conditions with the same maximum loads

Fibre type	Average strain to failure for a fatigue test of (0–57 cN tex^{-1})	Average strain to failure for a creep test with a constant load of 57 cN tex^{-1}
2 GTA	15.8 (±4.04) %	12.5 (±1.1) %
2 GTB	13.12 (±5.46) %	7.6 (±1.0) %

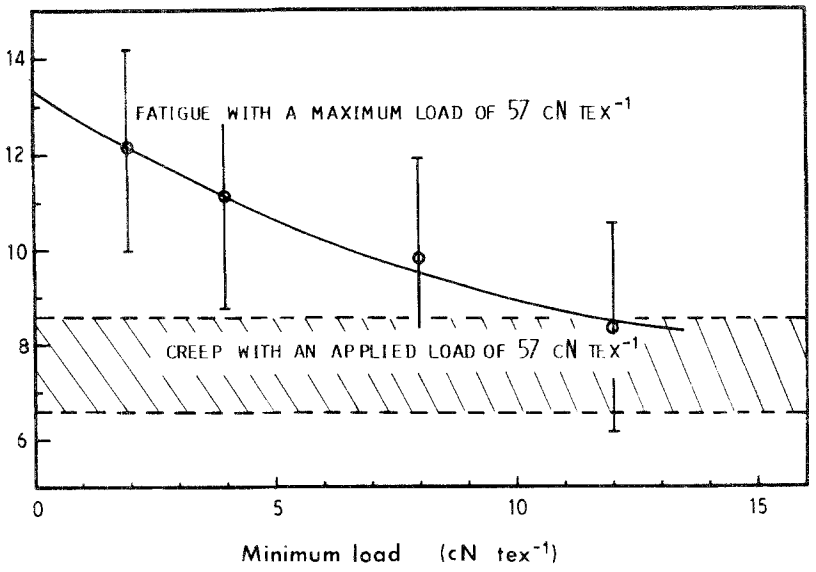

Figure 12 Comparison of strains to failure of fibres subjected to steady creep loading and to fatigue loading.

fatigue lives than the 2 GTA fibres despite having poorer creep behaviour. This can be understood as the 2 GTB fibres had a higher density of mesomorphous molecules which would have restricted molecular movement and restructuring. This suggests that it is the possibility of molecular movement within the fibre which determines fatigue behaviour. This hypothesis is supported by the observation that fatigued fibres fail at greater strains than do fibres failed under creep loading as shown by Table V and Fig. 12. The minimum load criterion for fatigue failure can be seen therefore to be determined by the need for reorganization of the molecular structure. This reorganization becomes increasingly difficult as the minimum cyclic load is increased which leads to longer lifetimes and the minimum load threshold level above which fatigue is not observed and creep processes dominate. The minimum load threshold level for fatigue was found to be different for the two types of fibres tested. The 2 GTB fibres were found to have a significantly lower threshold level than the 2 GTA fibres indicating again that the high density of the mesomorphous phase of the 2 GTB fibres inhibited molecular movement and fatigue as the minimum load was increased.

It seems likely therefore that fatigue lifetime is largely controlled by the initiation phase and that the fibre structure undergoes reorganization before a crack develops. Fig. 15 shows the surface of a fibre

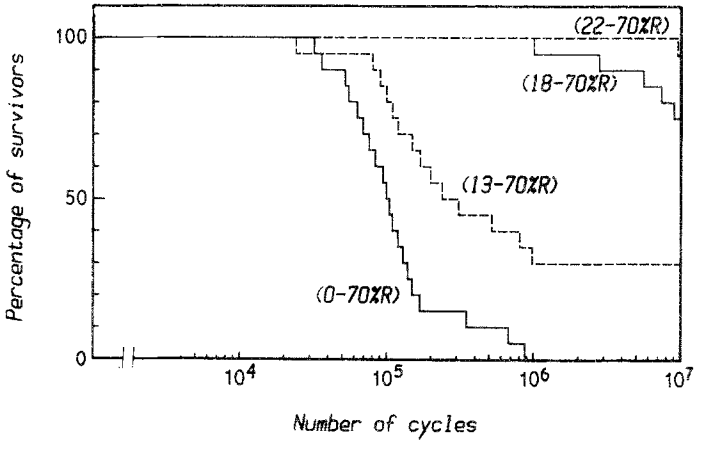

Figure 13 Cumulative histograms of fatigue lifetimes showing the influence of the minimum load.

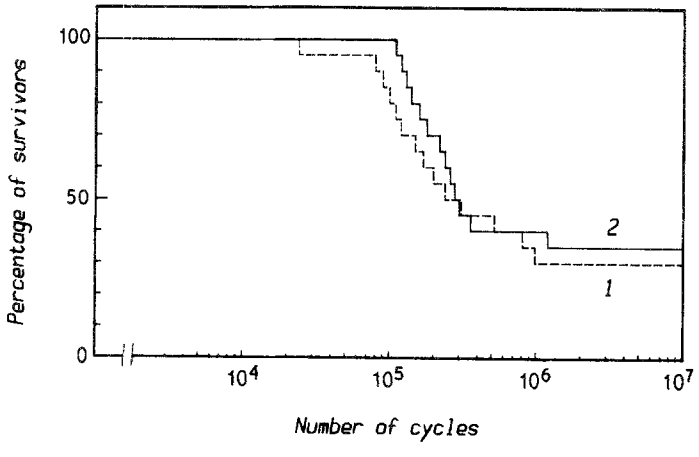

Figure 14 Cumulative histograms of fatigue lifetimes giving the same median lifetimes for the two fibres showing the effect of minimum load. (1) 2 GTA (11–57 cN tex^{-1}) (2) GTB (2–57 cN tex^{-1}).

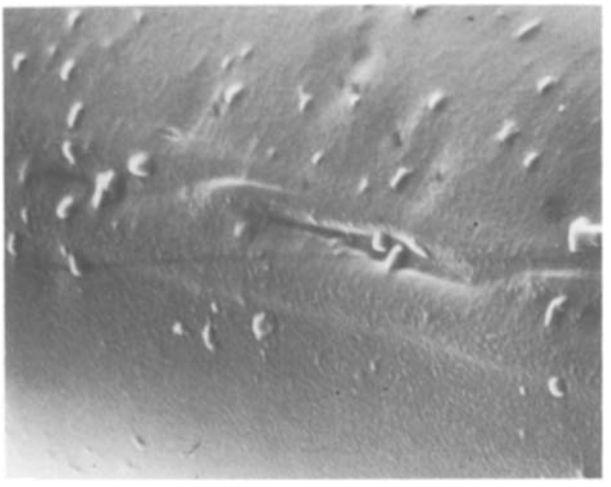

Figure 15 Surface modification revealing internal structural changes occurring during fatigue.

which had been subjected to several tens of thousands of load cycles under conditions which it was known would eventually lead to fatigue cracking. No fatigue crack was observed when the fibre was examined under SEM, however modification of the fibre surface indicating internal reorganization was observed. This type of surface irregularity was not seen with other fibres which had been subjected to loading which did not lead to fatigue.

5. Conclusion

The mechanisms involved in controlling the behaviour of polyester fibres under various tensile loading conditions have been determined. Fibres showing the best behaviour under simple tensile or creep loading conditions should be made up of large crystallites to which a maximum number of mesomorphous molecules should be attached.

The fatigue failure of polyester fibres requires the reorganization of the molecular structure, the effects of which can sometimes be seen on the fibre surface as a localized irregularity. The reorganization is rendered more difficult if the mesomorphous phase is dense and this results in a low minimum load threshold level above which fatigue does not occur. The structural modifications which occur lead to the development of an amorphous zone which develops along the fibre working gradually in towards the fibre centre in an irregular manner depending on the macromolecular fibre make-up. The fatigue crack would therefore appear to be the last stage of fatigue damage and result from the earlier molecular structural changes.

References

1. J. W. S. HEARLE and E. A. VAUGHN, *Rheol. Acta,* **9** (1969) 76.
2. D. C. PREVORSEK and W. J. LYONS, *Rubber Chem. Techn.*, **44** (1971) 271.
3. A. R. BUNSELL and J. W. S. HEARLE, *J. Mater. Sci.* **6** (1971) 1303.
4. *Idem, J. Appl. Polym. Sci.* **18** (1974) 267.
5. Ch. OUDET and A. R. BUNSELL, *J. Mater. Sci. Letters* **3** (1984) 295.
6. Ch. OUDET, A. R. BUNSELL, R. HAGEGE and M. SOTTON, *J. Appl. Polym. Sci.* **29** (1984) 4363.
7. J. DERMINOT, *Indus. Tex.*, No. 1083, (Nov. 1978).
8. A. R. BUNSELL, J. W. S. HEARLE and R. D. HUNTER, *J. Phys. E* **4** (1971) 868.
9. A. PETERLIN, *Tex. Res. J.*, p. 20 (Jan. 1972).
10. D. C. PREVORSEK and Y. D. KNOWN, *J. Macro. Sci. Phys.* **B12** (1976).
11. M. SOTTON, A.S.C. Symposium series No. 141, p. 193–213, (1979).
12. M. SOTTON, A. M. ARNIAUD and C. RABOURDIN, *Bull. Scient. Institut Textile de France* **7** (1978) 2165.
13. W. RULAND, *Acta. Crystall.* **14** (1961) 1180.
14. W. O. STATTON, *J. Appl. Polym. Sci.* **7** (1963) 803.
15. Von W. PECHHOLD and S. BLASENBREY, *Kolloid-Z u. Z Polymere* **241** (1970) 975.
16. T. C. CHIANG and J. P. SIBILIA, *J. Polym. Sci., Polym. Phys. Edn*, **10** (1972) 2249.

Received 25 November 1986
and accepted 29 January 1987